S1. Supplementary Figures

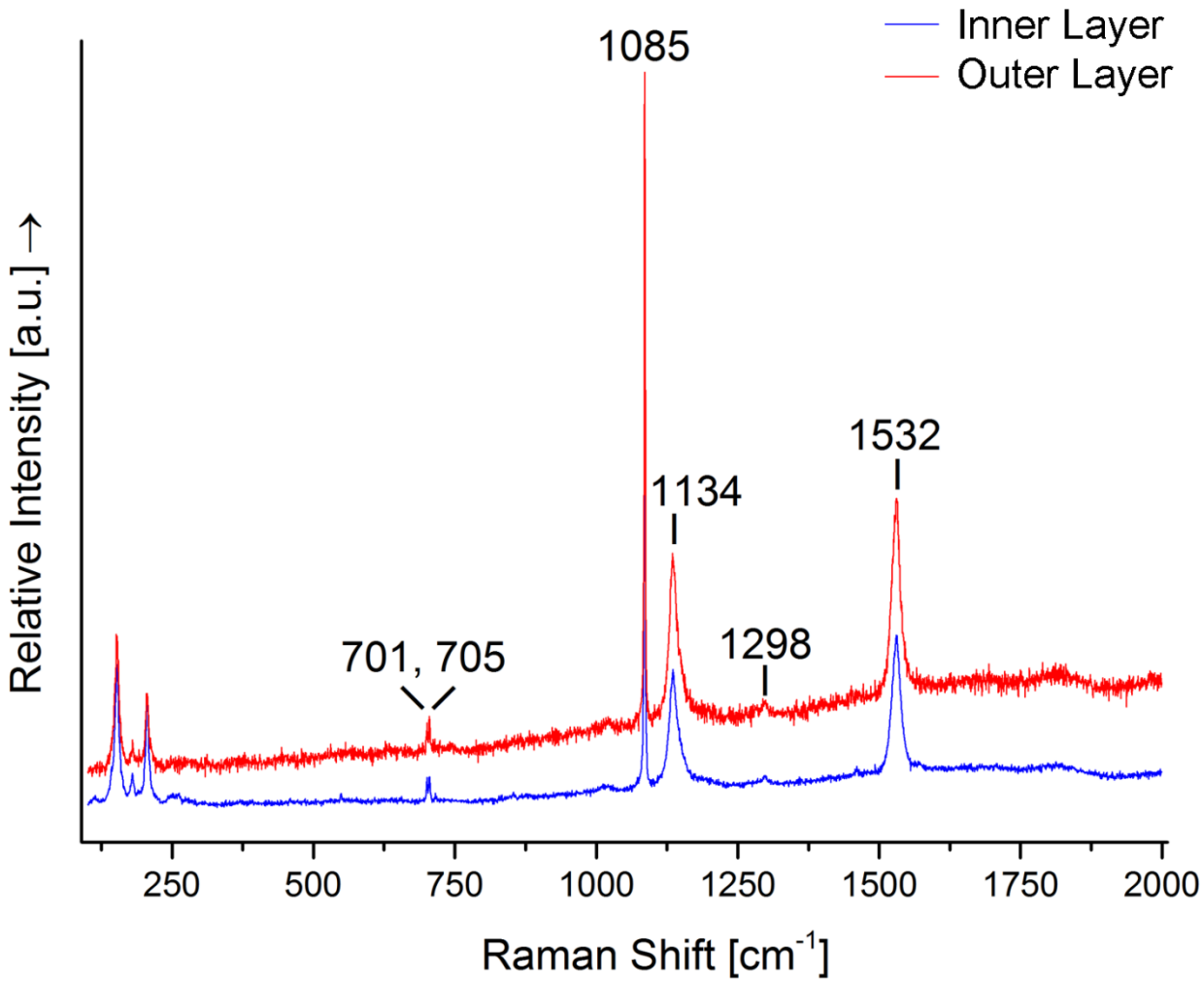

Figure S1: Representative micro-Raman spectra obtained from the inner and outer layer of a *K. rhytiphora* shell cross-section. Relative Raman intensities were normalized to the highest intensity peak, while no baseline correction was applied.

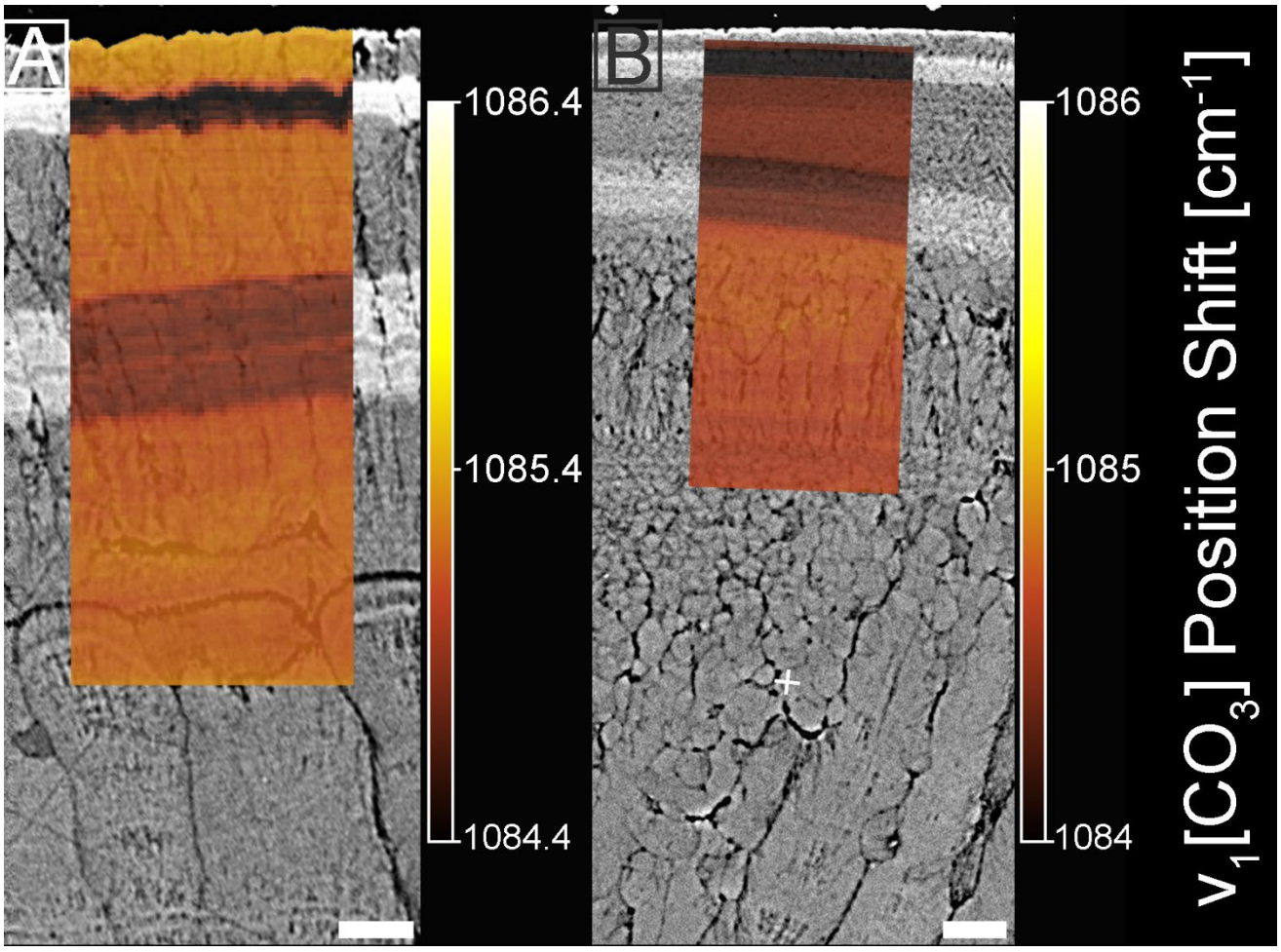

Figure S2: Micro-Raman maps obtained from a polished cross-section of a Sr-labelled *K. rhytiphora* showing the effect of variable Sr concentrations on the peak position of ν_1 located at 1084.8 cm^{-1} in the outer compound composite prismatic (A) and the inner crossed acicular layers (B) (see scale). All cross-sections in this supplement are prepared as radial sections along the maximum growth axis unless otherwise specified. Micro-Raman maps are overlain on BSE images. Lighter grey areas contain elevated Sr-contents (confirmed by nanoSIMS and EPMA) and show excellent correlation with position shifts to lower wavenumbers of about 0.5 cm^{-1} in the labelled shell layers. Scale bars are 10 µm.

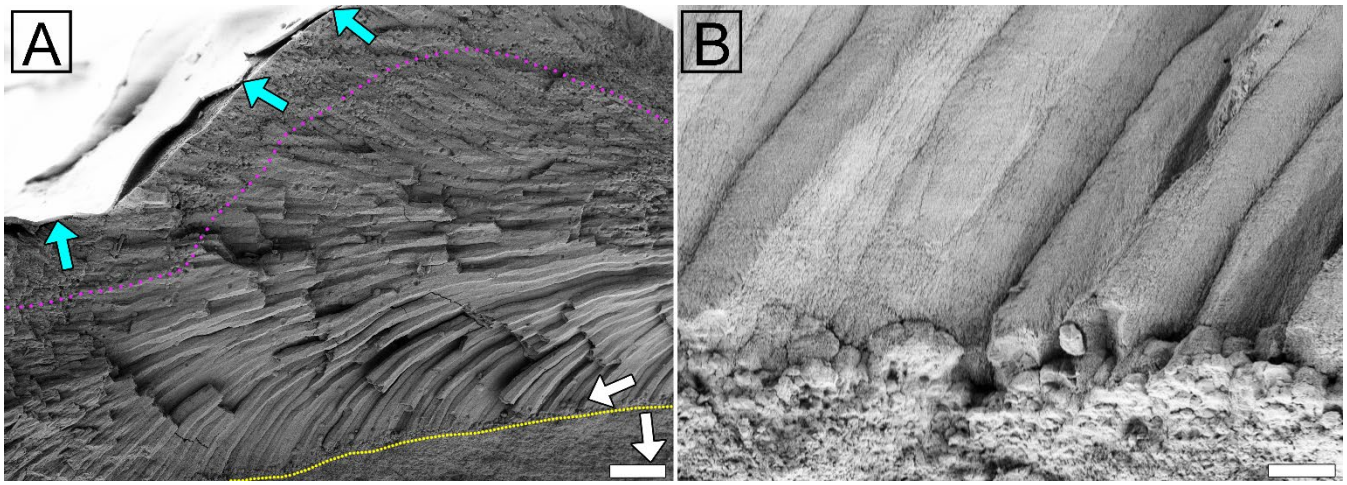

Figure S3: SE-images of a broken unpolished radial cross-sections of *K. rhytiphora*. Blue arrows in (A) point to well preserved areas of the thin periostracum layer, which measures about 1 µm in thickness. The purple dashed line marks a ca. 100 µm wide zone of spherulitic aragonite grains just underneath the periostracum. The yellow dashed line marks the boundary between the outer compound composite prismatic and inner crossed acicular ultrastructure with white arrows indicating the direction of growth for each ultrastructure. Magnification of the boundary between both layers (B) shows spherulitic grains of up to 8 µm in diameter o. Scale bars are 100 µm (A) and 10 µm (B).

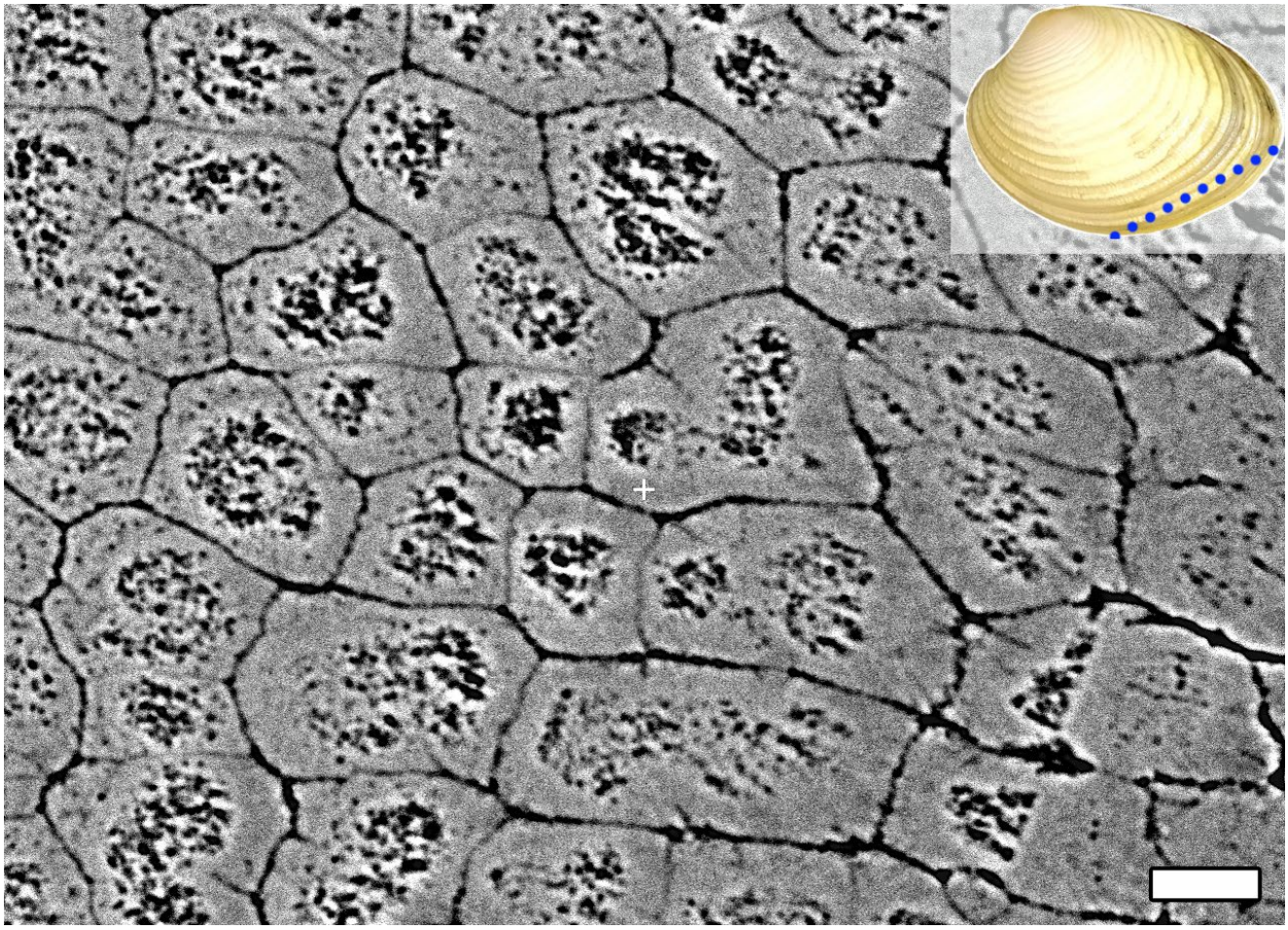

Figure S4: BSE image of a polished longitudinal cross-section of a *K. rhytiphora* shell. This orientation allows to observe first-order prisms perpendicular to their length axis (see sectioning plane indicated by blue dashed line in inset) for thickness measurements that average 17 ± 5 µm (n=20). Prism centres appear dark and patchy, which results from the angled, 3D radial arrangement of second-order prisms, some of which are removed during polishing. Scale bar is 10 µm.

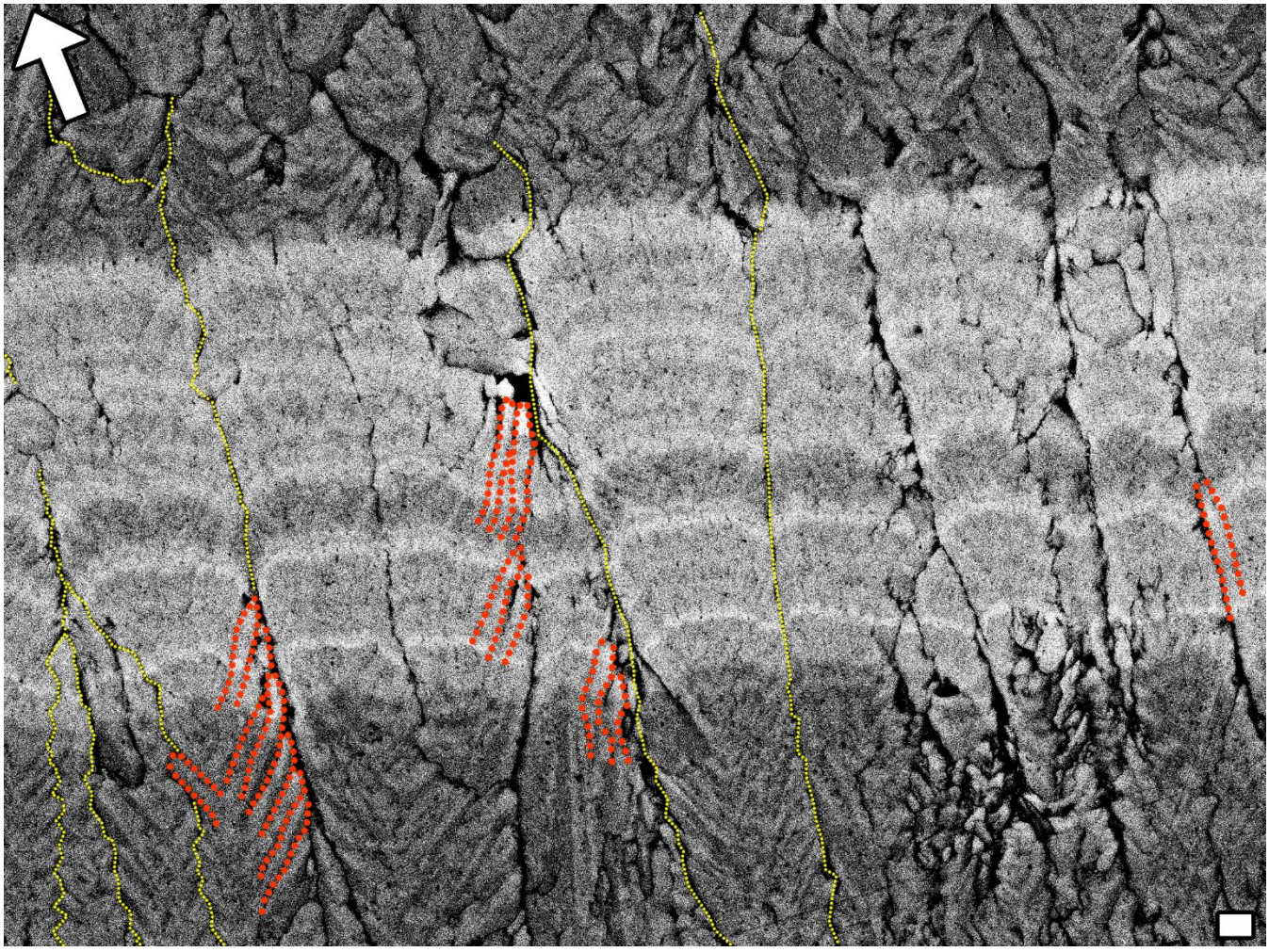

Figure S5: BSE image showing a polished cross-section of the innermost (first) Sr-label (LE1) in the compound composite prismatic ultrastructure (sample K2-04). The Sr-label appears as brighter grey due to a higher Z-contrast. First-order prisms (some outlined by yellow dashed lines) are separated by organic sheaths visible as dark grey. Second-order prisms (some outlined in red) radiate from the central axis of first-order prisms and have lengths and widths of 3 ±0.3 µm and 0.3 ±0.06 µm (n=8). However, these values are minimum values, since the base of each second-order prism is overlain by others. True lengths can be up to twice the measured values. The angle between two second-order prisms facing each other is 68°. The thickness of the 6 day Sr-label of 14 µm means that second-order prisms form in approx. 1.3 days during our experiments. The direction of shell growth is indicated by a white arrow. Scale is 1 µm.

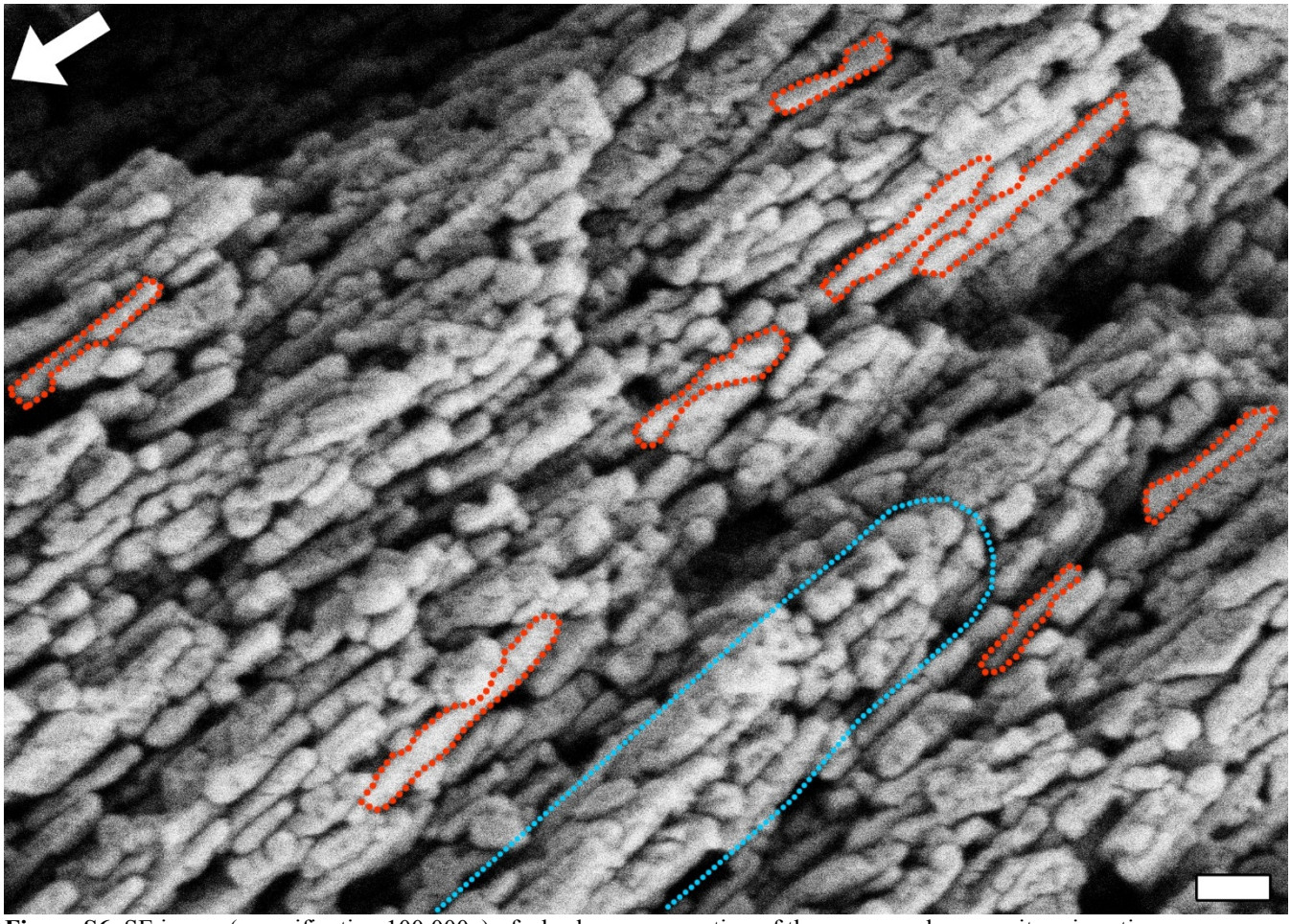

Figure S6: SE image (magnification 100,000x) of a broken cross-section of the compound composite prismatic ultrastructure (outer shell layer). Third-order prisms (some outlines in red) are orientated parallel to each other within second-order prisms (one outlines in blue). Fully exposed and unbroken third-order prisms were measured using ImageJ and have lengths and widths of approx. 496 ±129 nm and 67 ±16 nm (n=8), respectively. These prismatic units are 28x shorter than the Sr-labelled area of 14 µm, resulting in a growth rate of five third-order prisms per day during our experiments. White arrow indicates the direction of growth. The scale bar is 200 nm.

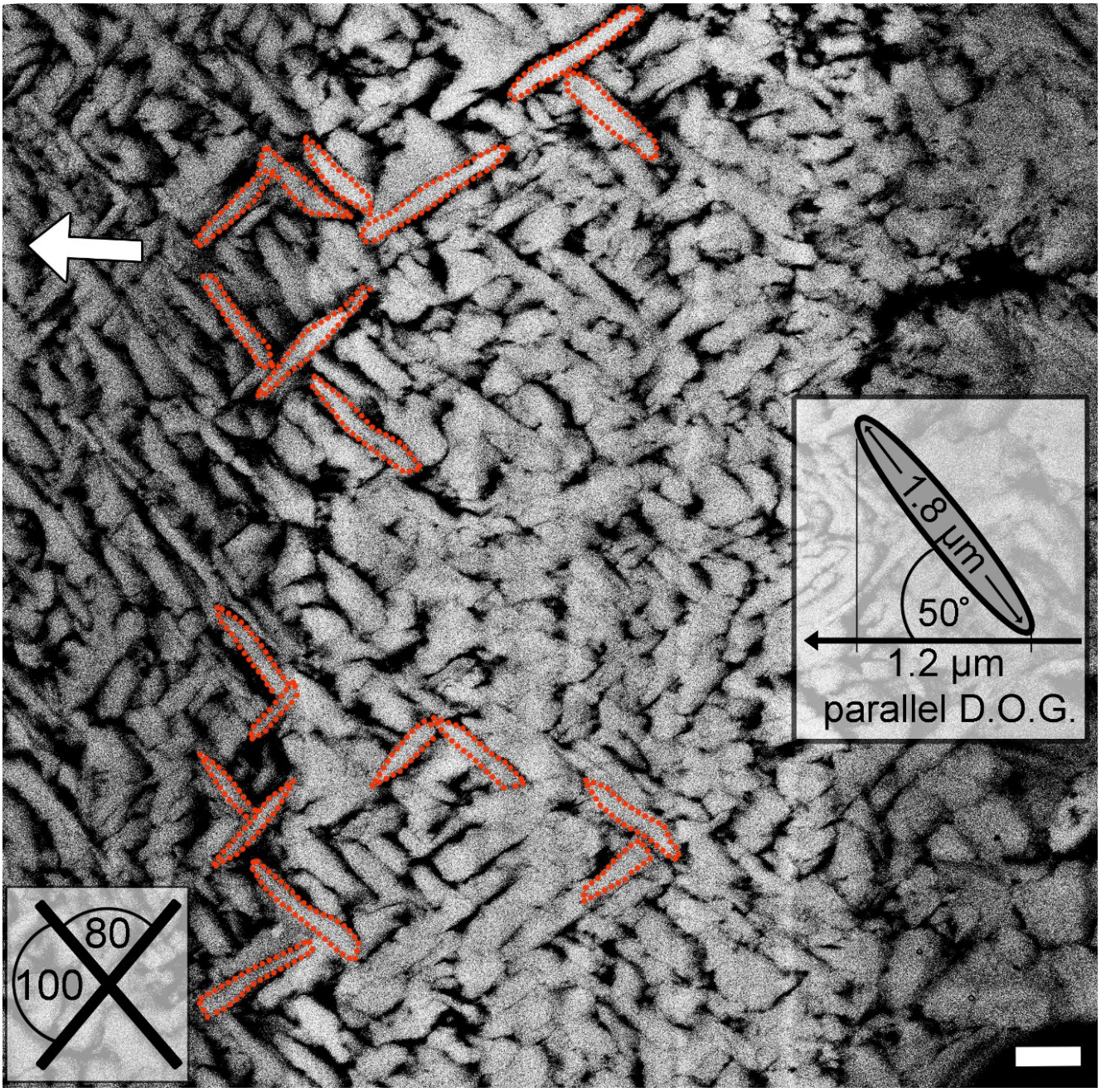

Figure S7: BSE image showing a polished cross-section of Sr-label (LE1) of the inner layer (crossed acicular ultrastructure) (sample K2-04). This structure consists of elongated lamellae (some outlines in red) arranged into intersecting bundles. Lengths and widths are 1.8 ± 0.4 µm and 0.22 ± 0.05 µm (n= 19), respectively, with an angle of 81°± 8° (n= 6). The projected length parallel to the direction of growth (D.O.G.) was calculated to be 1.2 µm (inset). Using the relationship between the projected length of 1.2 µm and the thickness of the LE1 label in this area (=9 µm) it can be estimated that acicular lamellae are deposited by a rate of 1 lamellae/day during our experiments. The white arrow indicates the direction of growth, scale bar is 1 µm.

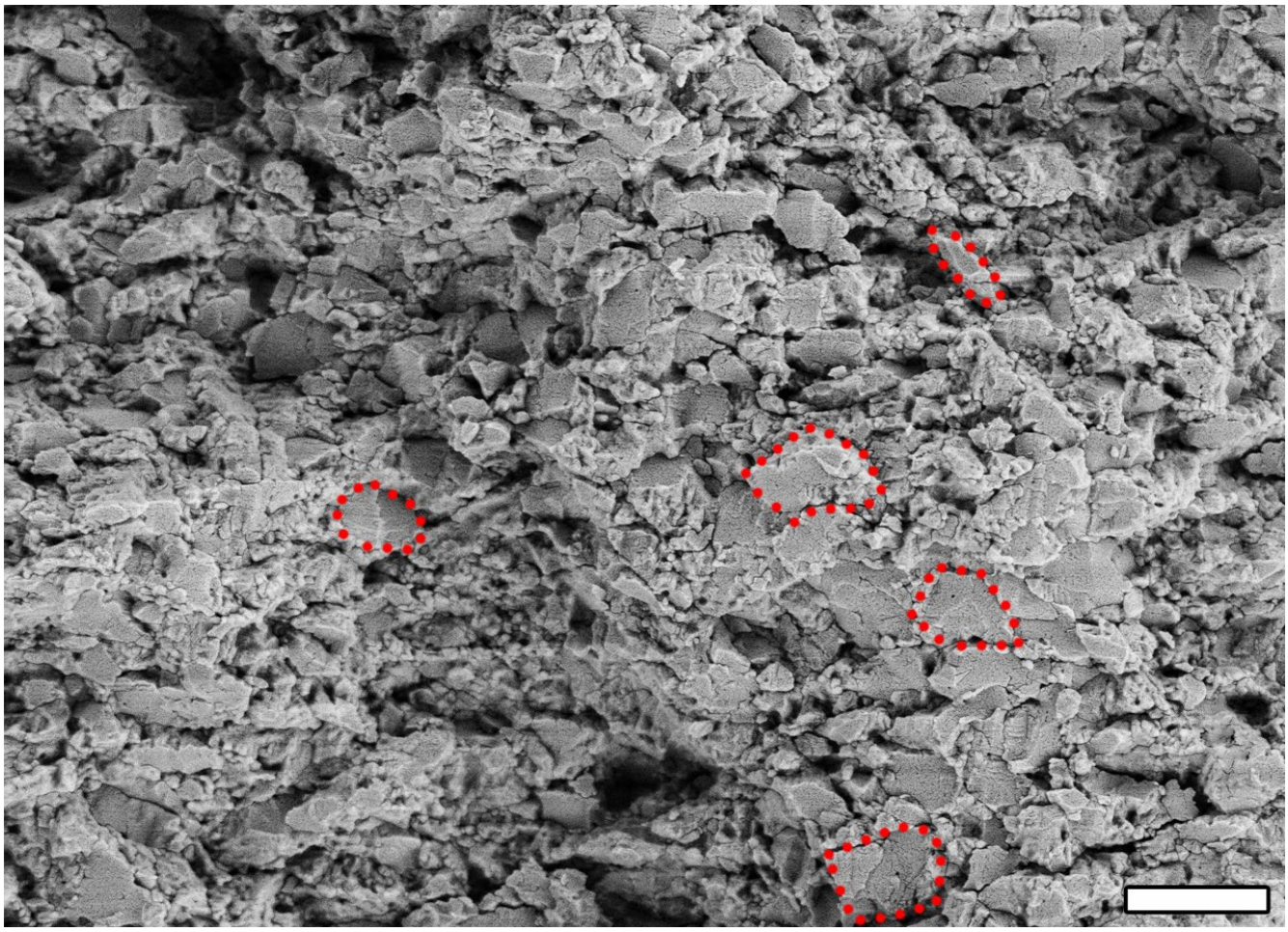

Figure S8: SE image showing an unpolished cross-section of the crossed acicular ultrastructure (inner shell layer). In contrast to BSE images, the crossed acicular units appear not as individual lamellae but rather as bundles of lamellae. This difference arises from the BSE image showing the organic scaffolds around the individual lamellae as darker greyscaled outlines, thus, visually separating the individual lamellae. The SE image does not reveal these chemical differences and shows the co-orientated groups of fused lamellae. The fused bundles have sizes of around 1.4 x 0.8 x 0.2 μm^3 (see one outlined by red dashed line). Scale bar is 2 µm.

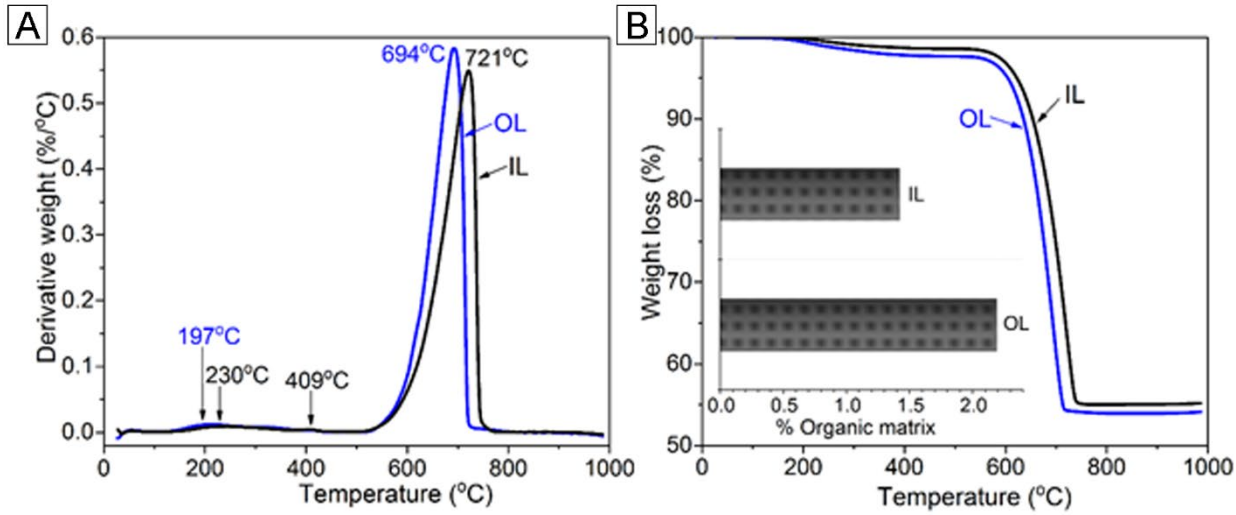

Figure S9: Differential thermal analysis (A) and thermal gravimetric analysis (B) show thermal stability and total organic matrix contents of inner- (IL) and outer- (OL) layer of *K. rhytiphora* shells. Considering the inorganic CO_2 content of 42-43% wt. % the organic matrix amounts to 1.42 wt.% for the inner shell layer consisting of crossed acicular ultrastructure and 2.19 wt.% for the outer compound composite prismatic layer (inset in (B).

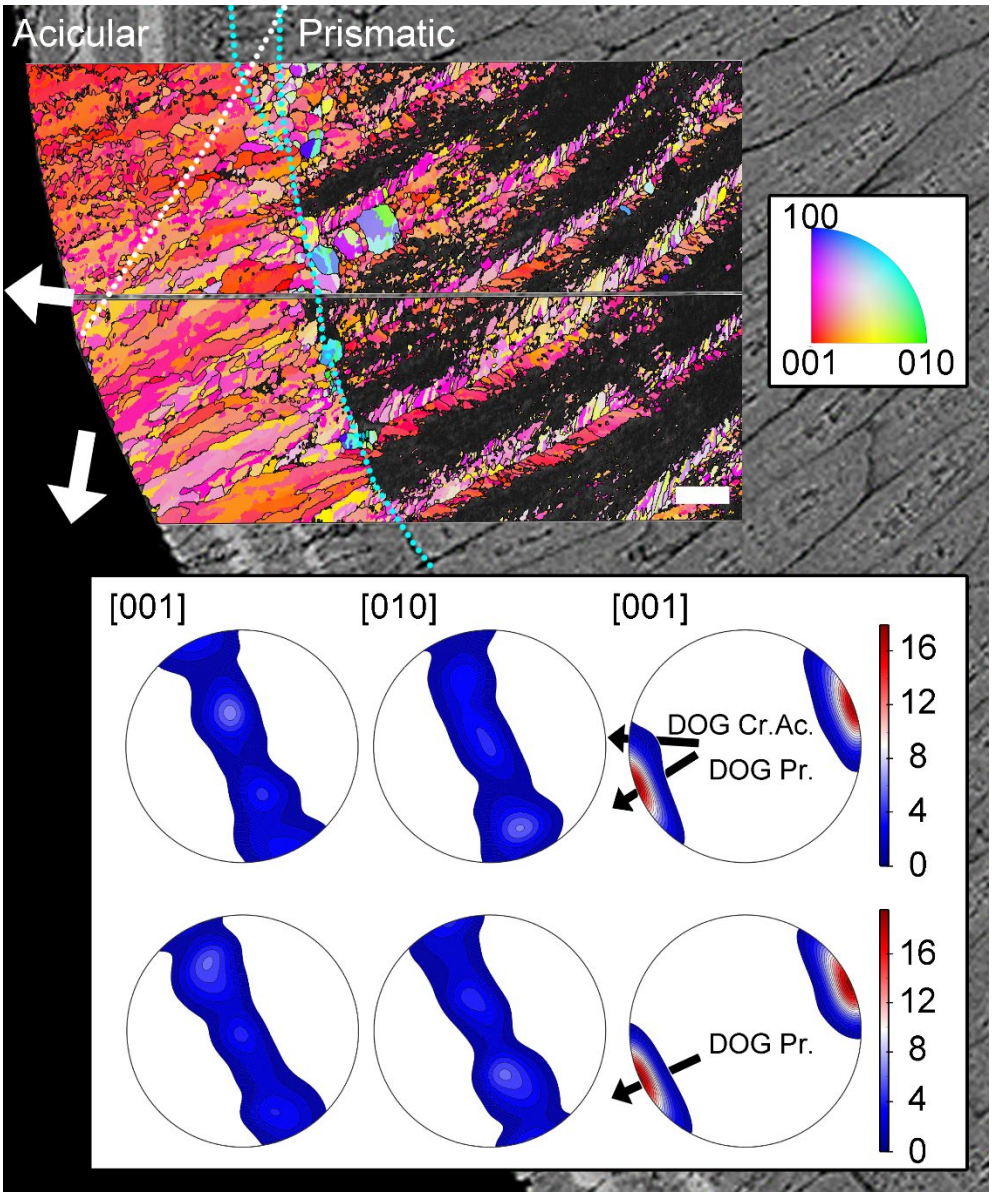

Figure S10: Orientation map for aragonite (A) of a pulsed Sr-labelled K. rhytiphora shell (specimen ID: K2-11). The map is color-coded using the inverse pole figure colouring scheme for orthorhombic aragonite: Blue, green, and red indicate the alignment of crystallographic a- [100], b- [010], and c-axes [001], respectively. The map is color-coded to show which crystallographic axis is aligned parallel to the growth direction of the shell-layers. The predominance of red color shades indicates that the crystallographic c-axis [001] is well aligned parallel to the growth directions. The dotted white line follows the acicular-prismatic boundary between inner and outer shell layers. Second-order prisms appear feathery arranged within first-order prisms. Core areas of first-order prisms remain dark and unindexed likely as an effect of polishing (see main text). The organic growth check in the outer structure that transitions into a thin prismatic layer in the inner layer is highlighted with light blue dotted lines. Pole figures (lower hemisphere, equal area projection) show the mineral fabric for [100], [010] and [001] axes of aragonite and exhibit a strong cluster of [001] along the direction of growth for the prismatic section (DOG Pr.). In the [100] and [010] directions the data forms a girdle of random orientations that corresponds to the direction of the growth lines running perpendicular to the direction of shell growth. In the upper pole figure row that's been derived from the

upper EBSD map, a small contribution of the inner crossed acicular structure is observed (DOG Cr. Ac.) that is not present in the pole figures of the lower row (derived from the lower EBSD map). Maximum density values of pole figures are color coded according to scale bar with the [001] axes achieving 18.70 times uniform. Scale bar is 10 µm.

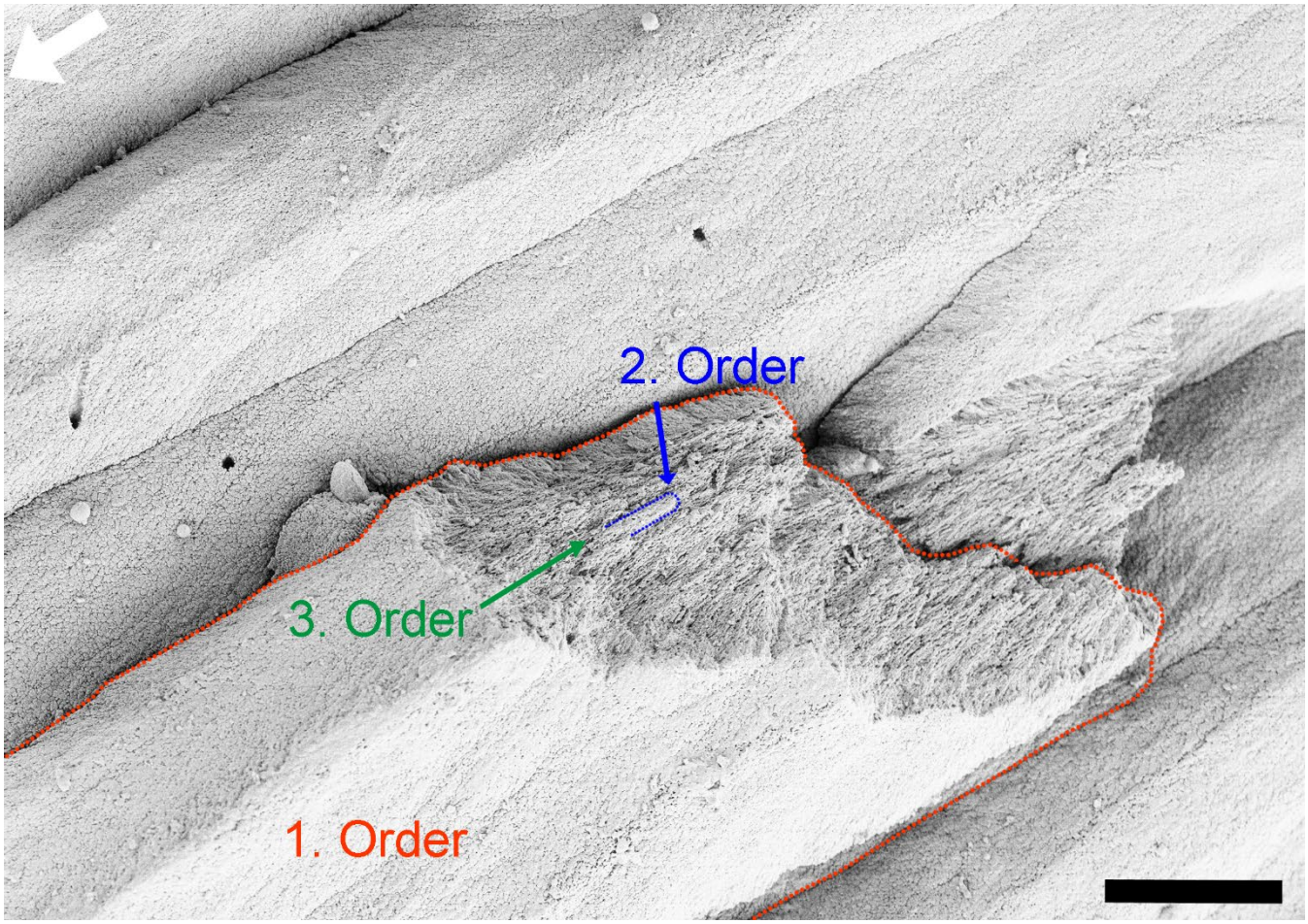

Figure S11: SE image showing a broken radial cross-section of the compound composite prismatic ultrastructure of a *K. rhytiphora*. First-order prisms (red outline), second-order prisms (blue outline) and third-order prisms (as fine-grained texture) are visible. The white arrow indicates the direction of growth. Scale bar is 10 µm.

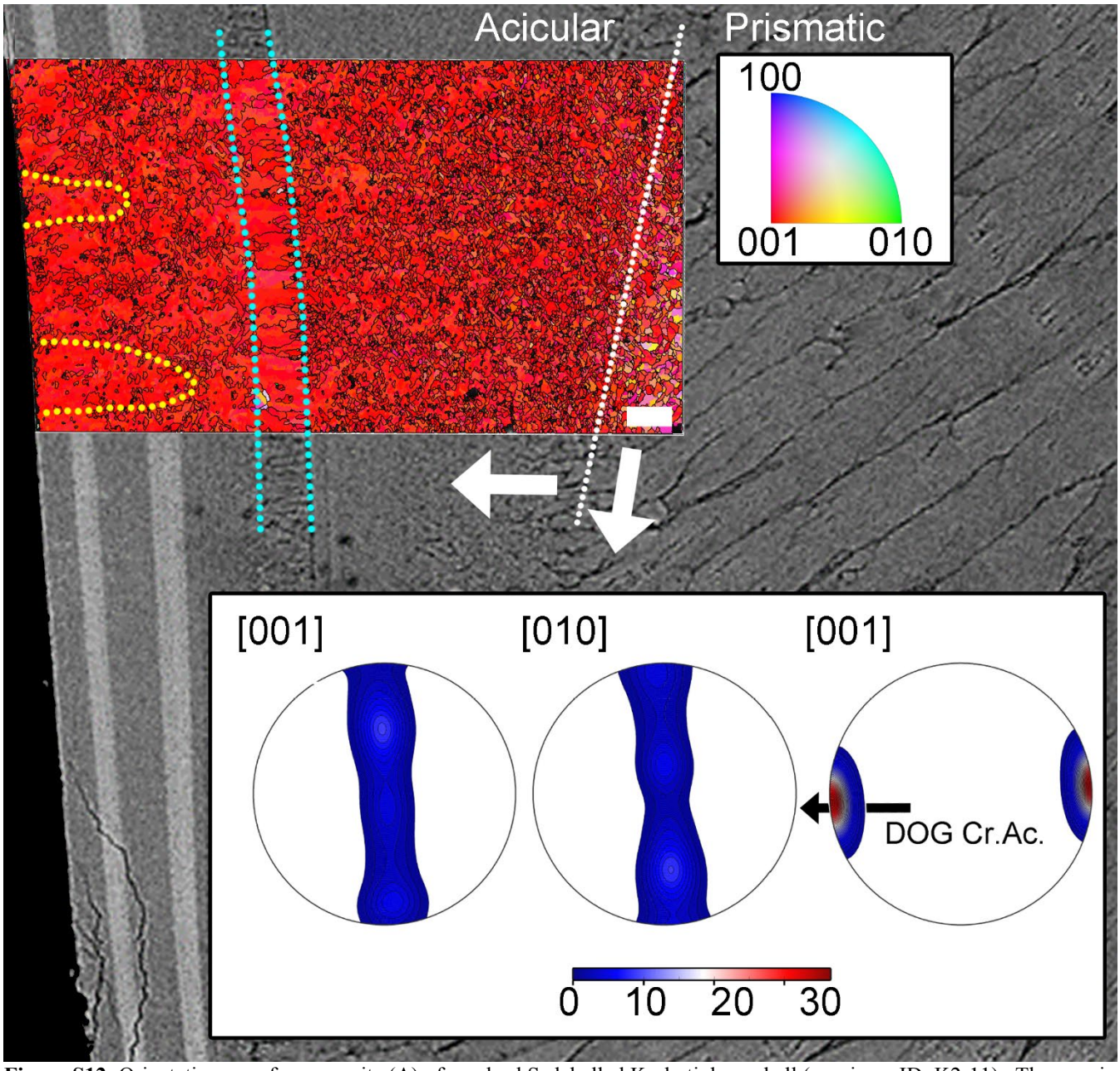

Figure S12: Orientation map for aragonite (A) of a pulsed Sr-labelled K. rhytiphora shell (specimen ID: K2-11). The map is color-coded using the inverse pole figure colouring scheme for orthorhombic aragonite: Blue, green, and red indicate the alignment of crystallographic a- [100], b- [010], and c-axes [001], respectively. The map is color-coded to show which crystallographic axis is aligned parallel to the growth direction of the shell-layers. The predominance of red color shades indicates that the crystallographic c-axis [001] is well aligned parallel to the growth directions. The boundary between inner crossed acicular and outer compound composite prismatic shell layers is marked by a dashed white line. Two dashed light blue lines highlight the thin prismatic layer that continues from the organic growth check within the outer layer. At the inner shell surface, the crossed acicular structure shows crystallographic co-orientated areas (yellow outlined that might resemble pseudo-prisms (Pérez-Huerta et al., 2014). Pole figures (lower hemisphere, equal area projection) show the alignment of the

EBSD data with the [100], [010] and [001] directions of aragonite and exhibit a strong crystallographic preferred orientation (CPO) of the [001]. The area of highest data density (red) aligns well with direction of growth of the crossed acicular ultrastructure (DOG Cr. Ac.). In the [100] and [010] directions the data forms a narrow girdle of random orientations that corresponds to the direction of the growth lines running perpendicular to the direction of shell growth. Maximum density values of pole figures are color coded according to scale bar with the [001] axes achieving 36.49 times uniform, which exceeds significantly the value of the outer prismatic structure. Scale bar is 10 μm.

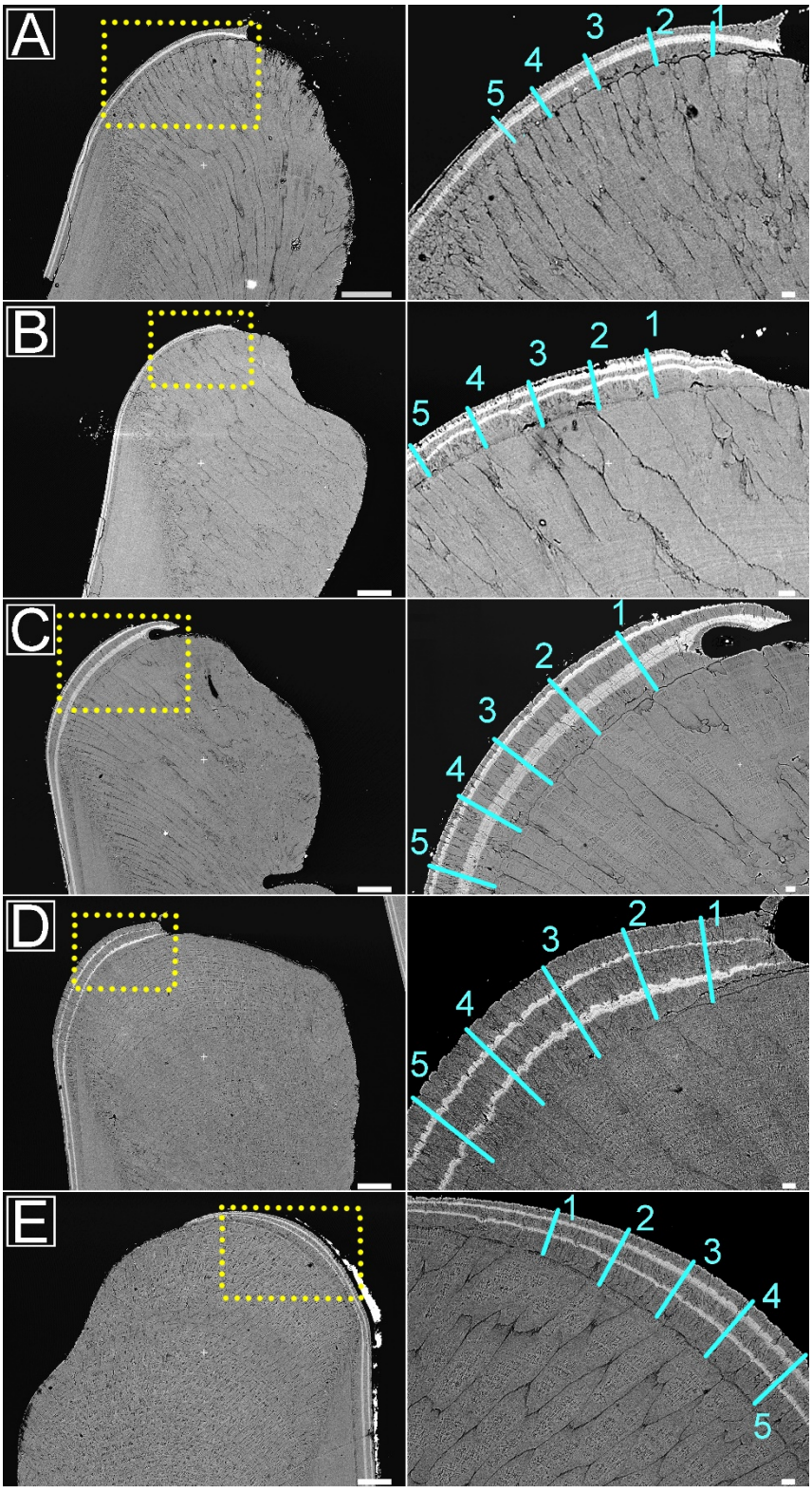

Figure S13: BSE images of polished cross-sections of compound composite prismatic shell at the calcification front of the ventral margin. Overview images (left side) as well as higher magnification images of areas marked in yellow (right side) show the Sr-labels along the growth fronts. Blue, numbered lines indicate where calcification rate measurements were obtained (Suppl. Table 3, averages Table 2, main text). Specimens used are K2-01 (A), K2-02 (B), K2-04 (C), K2-08 (D) and K2-11 (E). Specimens K2-06, K2-10 and K2-14 are excluded here as they showed different perturbations at this growth front. Scale bars: 100 µm for all images on the left and 10 µm for images on the right.

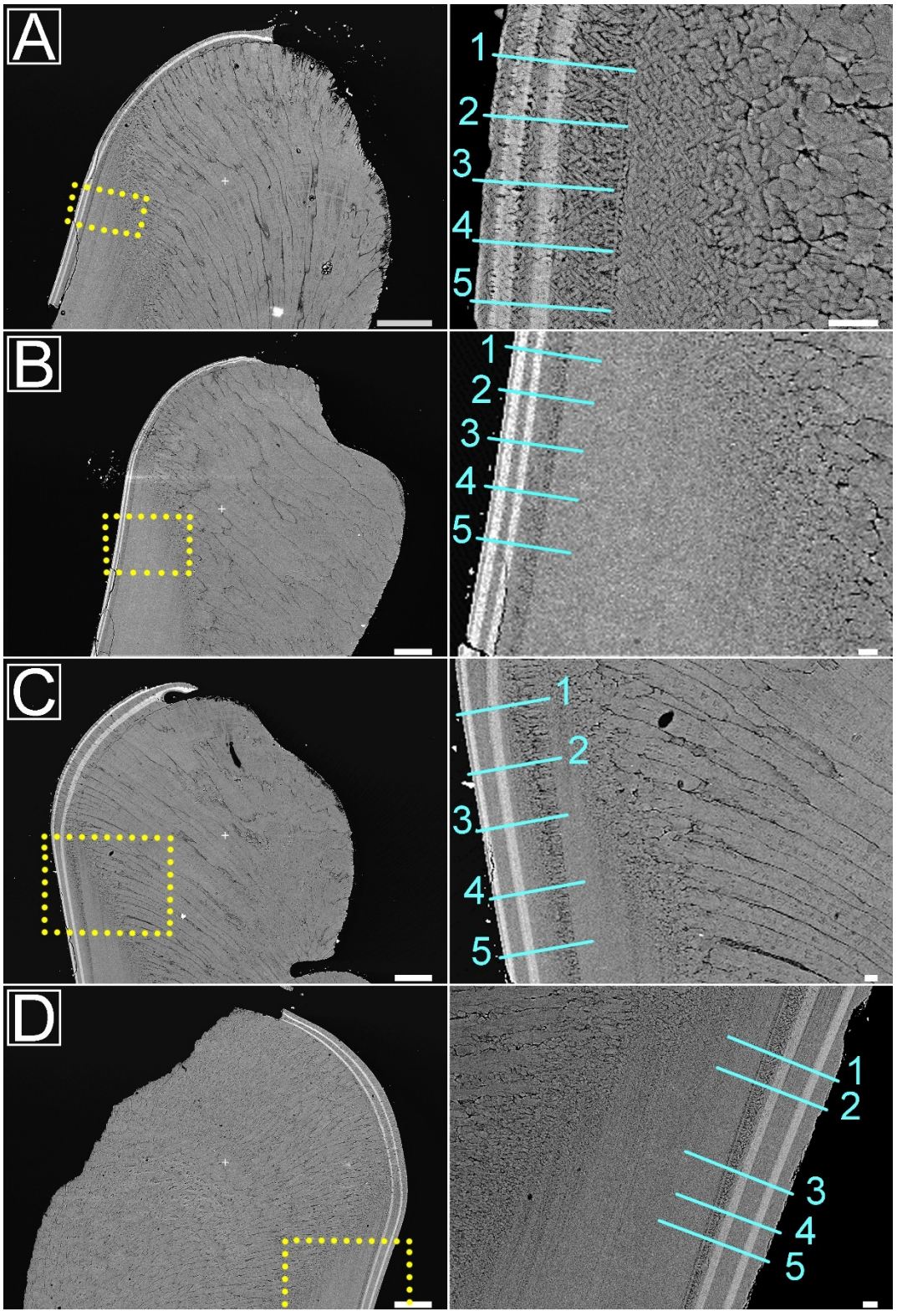

Figure S14: BSE images of polished cross-sections of crossed acicular shell near the calcification front of the ventral margin. Overview images (left side) as well as higher magnification images of areas marked in yellow (right side) show the Sr-labels along the growth fronts. Blue, numbered lines in the images on the right side indicate were growth measurements were obtained (Suppl. Table 4, averages Table 2, main text). Specimens used are K2-01 (A), K2-02 (B), K2-04 (C), K2-06 (D), K2-08 (E), K2-10 (F), K2-11 (G), and K2-14 (H). Scale bars: 100 µm for all images on the left and 10 µm for images on the right.

(Fig. S14 Continued)

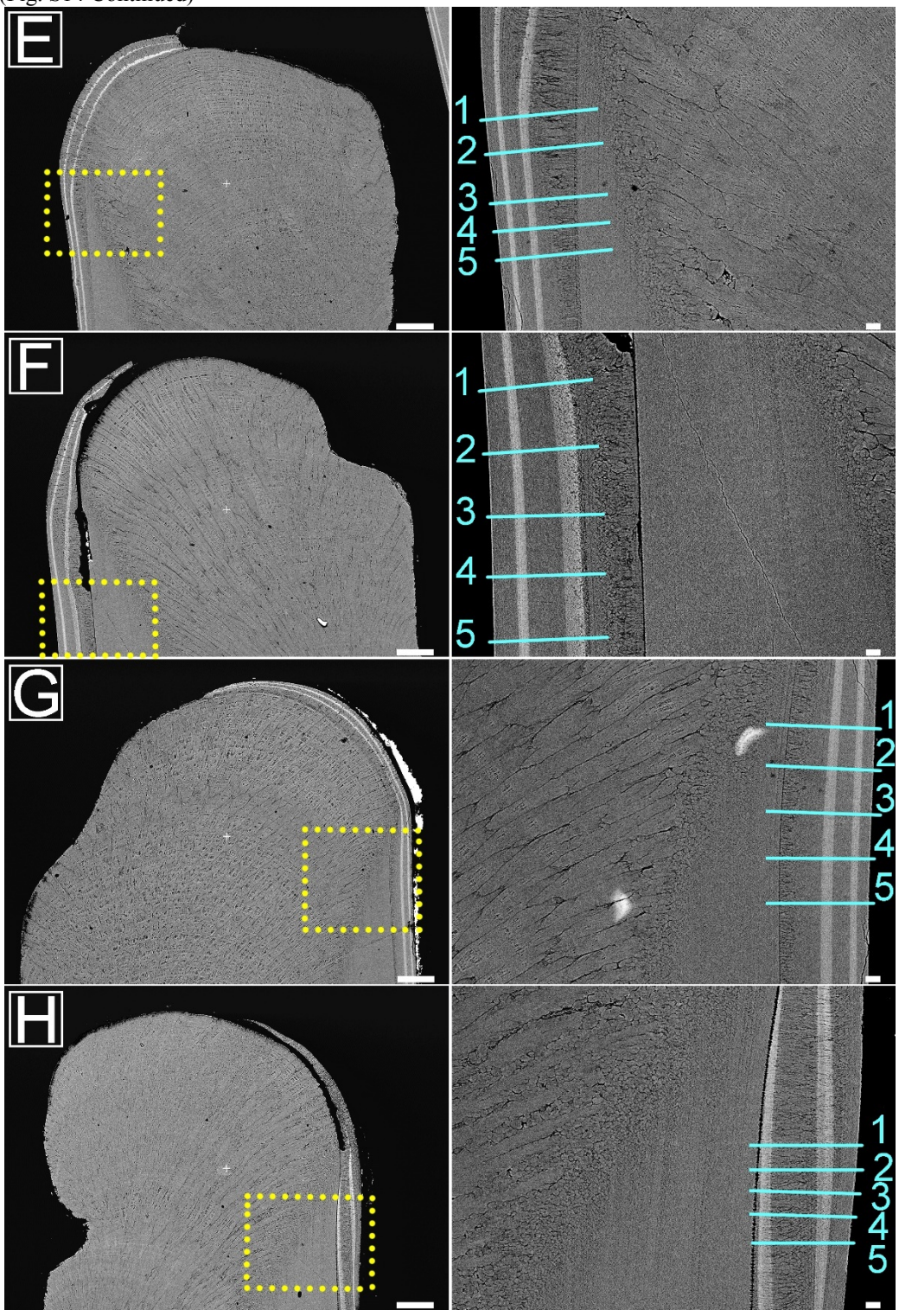

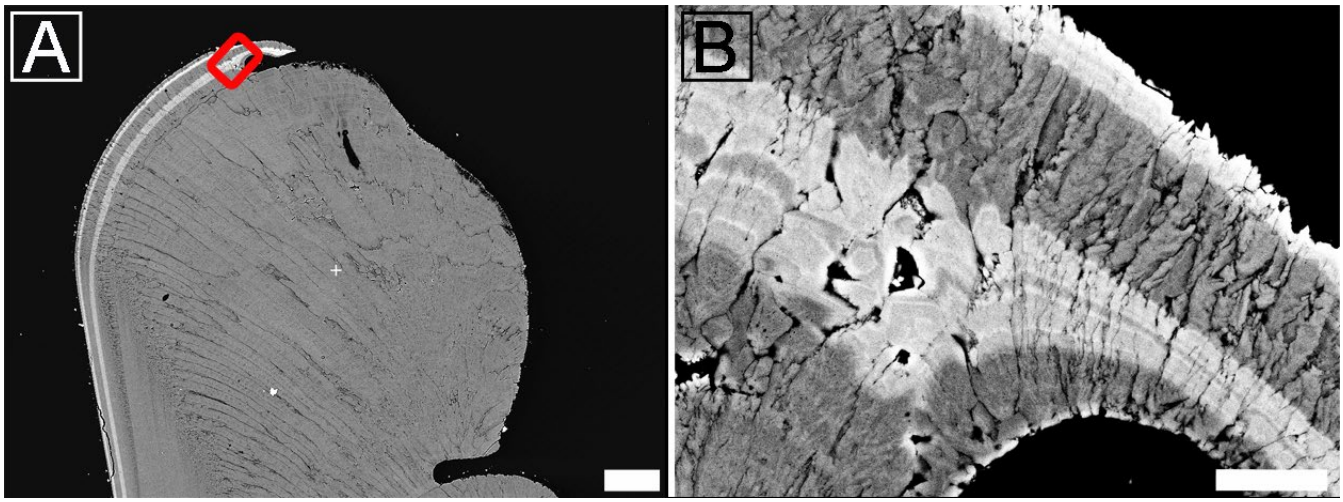

Figure S15: BSE images showing a polished cross-section (sample K2-04). (B) shows an enlarged area indicated by the red box in (A). It can be clearly seen how the new ridge feature formed as a consequence of very high short-term growth rates, likely, to stabilize the fragile new tip area. Scale bars are 100 µm (A) and 10 µm (B).

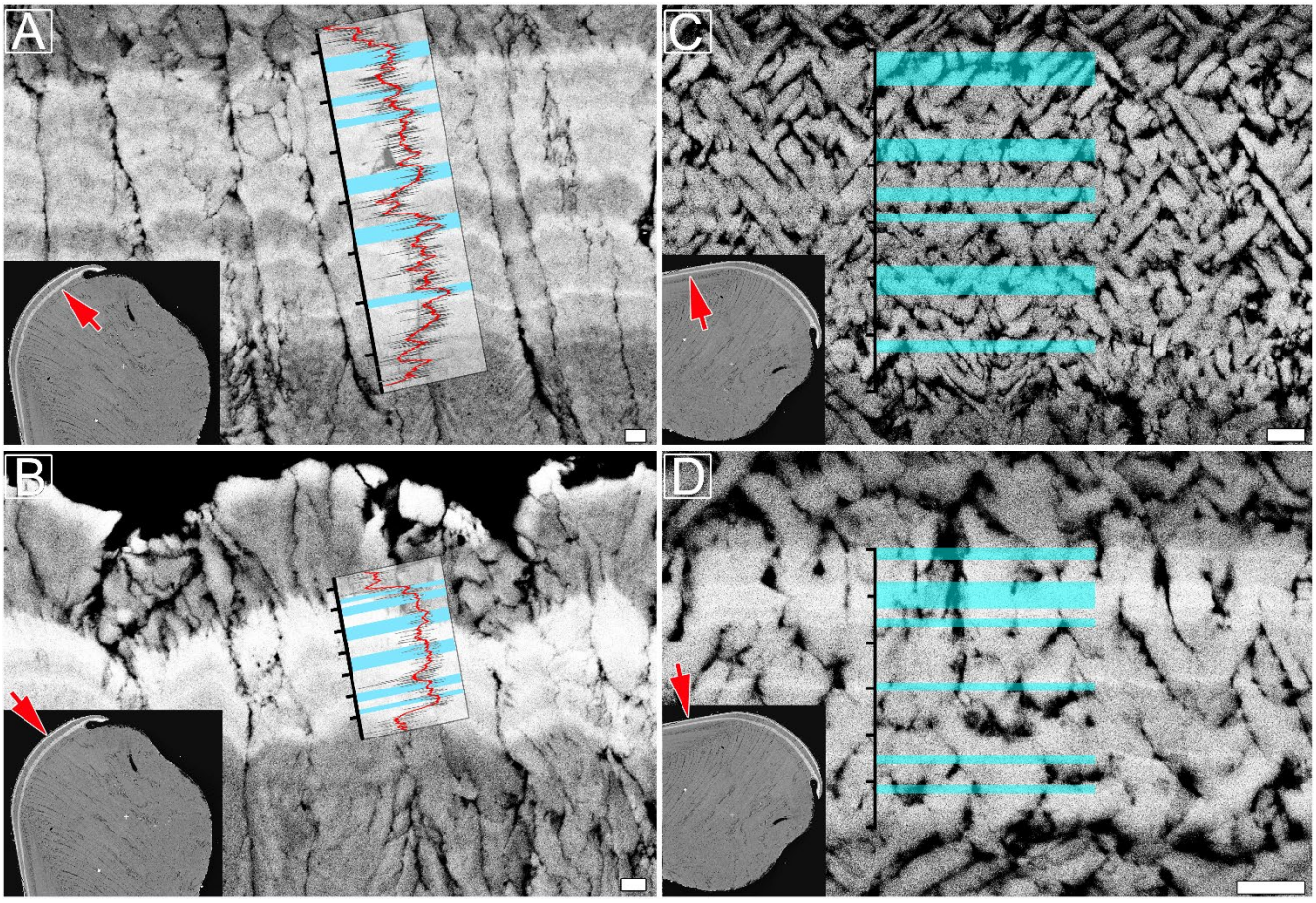

Figure S16: BSE images showing polished cross-sections of a Sr-labelled *K. rhytiphora* (sample K2-04). In the compound composite prismatic (outer) layer, both Sr-labels LE1 (A) and LE2 (B) consist of several narrow increments of varying bright greyscales. Similar patterns are observed in the crossed acicular (inner) layer for LE1 (C) and LE2 (D) Comparison with nanoSIMS (Fig. 2) and micro-Raman maps (Fig. 3) confirm true differences in Sr-incorporation between these micro-increments. Line profile insets of BSE greyscale intensities for LE1 (in A) reveals six distinct peaks with tick marks indicating the individual days spent in Sr-labelling conditions (and approx. six in LE2 (B)). Generally, brighter greyscale areas correlating with the peaks in the line scans are significantly thinner than the darker areas between them. Differences in intensity and width of increments observed within the labels are suggested to result from rhythmical metabolic activity with higher growth rates incorporating higher amounts of Sr (as peaks) followed by intervals of lower Sr concentration, due to lower growth rates. The crossed acicular ultrastructure (inner layer) shows similar patterns that are here highlighted by blue lines after visual examination as it is not possible to obtain line-profiles across these labels as the organic sheaths surrounding the lamellae distort the line profiles severely. Scale bars are 1 µm.

S2. Supplementary Tables

Table S1: WDX Electron Probe Micro Analyser (EPMA) "Biocarb" parameters.

Routine:	Biocarb:
Accelerating Voltage:	15 kV
Beam Current:	8 nA
Spot Size:	Scanning at 20000 magnification
Elements and lines used:	11
- Na Kα	Albite
- Mg Kα	Dolomite
- P Kα	Apatite
- S Kα	$BaSO_4$
- Cl Kα	Tugtupite
- K Kα	Orthoclase
- Ca Kα	$CaCO_3$
- Mn Kα	Rhodochrosite
- Fe Kα	Fe_2O_3
- Sr Lα	$SrSO_4$
- Ba Lα	$BaSO_4$

Table S2: Raman band parameters of $\nu_1[CO_3]$ as obtained from micro-Raman hyperspectral mapping of Sr-labelled and unlabelled aragonite of the outer compound composite prismatic and inner crossed acicular structure. FWHM distributions are shown in Fig. 3 of the main text, while Raman band positions shifts are shown in Supplementary Fig. 3. Averages from spectra within labelled and unlabelled sample regions (~ 25 µm²) are given (Ø) together with minimum and maximum values of multiple spots (2.25 µm²) and reflect subtle changes within respective layers. All FWHM values were corrected following the equation of Váczi (2014).

	Sample Area:	FWHM [cm^{-1}]		Raman shift [cm^{-1}]	
Compound composite prismatic	LE 1	Ø	1.9	Ø	1084.5
		Max:	2.7	Max:	1084.8
		Min:	1.7	Min:	1084.6
	NL 1	Ø	1.7	Ø	1084.8
		Max:	1.8	Max:	1084.9
		Min:	1.6	Min:	1084.7
	LE 2	Ø	2.1	Ø	1084.4
		Max:	2.2	Max:	1084.5
		Min:	2.0	Min:	1084.3
	NE 2*		n.a.		n.a.
Crossed acicular	LE 1	Ø	1.8	Ø	1084.7
		Max:	1.9	Max:	1084.9
		Min:	1.7	Min:	1084.6
	NL 1	Ø	1.5	Ø	1085.3
		Max:	1.6	Max:	1085.4
		Min:	1.4	Min:	1085.2
	LE 2	Ø	2.3	Ø	1084.5
		Max:	2.4	Max:	1084.6
		Min:	2.2	Min:	1084.4
	NE 2	Ø	1.5	Ø	1085.3
		Max:	1.5	Max:	1085.4
		Min:	1.3	Min:	1085.2

*NL 2 in the crossed acicular ultrastructure map was here too narrow for measuring.

Table S3: Calcification rates (three replicate measurements) under pulsed Sr-labelling aquaculture conditions for the outer layer of *K. rhytiphora*. Line # refer to blue, numbered lines in Supplementary Fig. 13 where growth measurements were obtained. LE 1 and LE 2 (both 6 days), refer to the first and second labelling periods while NE 1 (12 days) depicts normal Sr conditions between LE 1, LE 2, and NE 2 (either *6 days* or 12 days depending on specimen) describes growth at normal conditions after the last labelling event. Specimens K2-06, K2-10 and K2-14 are excluded here as they showed different perturbations at this growth front.

Sample ID:	Line #:	Rep.:	LE 1 [µm/6d]	NE 1 [µm/12d]	LE 2 [µm/6d]	NE 2 [µm/*6d*] or [µm/12d]
(A) K2-01	1	A	5.23	5.97	0	*0*
		B	5.33	5.97	0	*0*
		C	5.34	5.76	0	*0*
	2	A	5.07	5.69	0	*0*
		B	5.20	5.72	0	*0*
		C	5.00	5.51	0	*0*
	3	A	5.97	5.39	0	*0*
		B	6.07	5.25	0	*0*
		C	5.96	5.11	0	*0*
	4	A	4.87	6.57	0	*0*
		B	4.68	6.75	0	*0*
		C	4.65	6.55	0	*0*
	5	A	4.48	5.13	0	*0*
		B	4.31	4.77	0	*0*
		C	4.38	4.98	0	*0*
		Ave.	**5.10**	**5.68**	**0**	***0***
		Stdev.	**0.55**	**0.58**	**0**	***0***
(B) K2-02	1	A	2.52	3.44	3.49	*3.02*
		B	2.52	3.46	3.50	*3.08*
		C	2.64	3.32	3.30	*2.93*
	2	A	2.62	4.19	2.60	*3.03*
		B	2.65	4.12	2.67	*3.18*
		C	2.64	4.09	2.70	*3.05*
	3	A	2.02	4.40	2.38	*2.83*
		B	1.98	4.34	2.47	*2.78*
		C	1.91	4.33	2.34	*2.85*
	4	A	2.07	3.06	2.02	*3.01*
		B	2.19	2.83	2.27	*2.93*
		C	2.07	2.94	2.07	*2.91*
	5	A	1.68	3.70	2.34	*2.29*
		B	1.77	3.68	2.34	*2.18*
		C	1.72	3.64	2.28	*2.21*
		Ave.	**2.20**	**3.70**	**2.58**	***2.82***
		Stdev.	**0.35**	**0.51**	**0.46**	***0.31***
(C) K2-04	1	A	15.03	19.12	6.00	*5.00*
		B	14.92	19.17	6.16	*5.20*
		C	14.97	19.32	6.09	*5.14*
	2	A	12.44	20.21	4.69	*7.24*
		B	12.75	20.61	4.51	*7.24*
		C	12.95	20.23	4.65	*7.04*
	3	A	13.11	19.53	4.33	*5.93*
		B	13.00	19.62	4.42	*5.74*
		C	13.11	19.60	4.01	*5.73*
	4	A	12.94	19.99	4.80	*5.68*
		B	13.04	20.16	4.78	*5.62*
		C	13.49	19.94	4.65	*5.49*
	5	A	12.47	20.89	4.47	*5.34*
		B	12.41	20.80	4.39	*5.02*
		C	12.46	20.49	4.40	*5.15*
		Ave.	**13.27**	**19.98**	**4.82**	***5.77***
		Stdev.	**0.90**	**0.56**	**0.66**	***0.75***

Table S3 continued.

Sample ID:	Line #:	Rep.:	LE 1 [μm/6d]	NE 1 [μm/12d]	LE 2 [μm/6d]	NE 2 [μm/*6d*] or [μm/12d]
(E) K2-08	1	A	5.76	21.47	2.17	16.59
		B	5.64	21.17	2.20	16.57
		C	5.65	21.15	2.12	16.45
	2	A	8.54	24.65	2.70	15.99
		B	8.52	24.53	2.77	16.21
		C	8.44	24.57	2.73	15.95
	3	A	8.89	22.21	4.16	17.30
		B	8.74	22.33	3.96	17.48
		C	8.03	22.30	4.11	17.12
	4	A	5.20	20.15	4.13	17.10
		B	5.13	20.07	4.43	17.32
		C	5.20	19.99	4.20	17.40
	5	A	4.30	23.46	4.21	17.33
		B	3.93	23.36	4.36	17.36
		C	4.12	23.58	4.28	17.51
		Ave.	**6.40**	**22.33**	**3.50**	**16.91**
		Stdev.	**1.81**	**1.59**	**0.89**	**0.54**
(F) K2-11	1	A	1.86	8.43	1.98	5.24
		B	1.80	8.53	2.06	5.40
		C	1.89	8.57	1.99	5.33
	2	A	3.28	10.30	2.99	7.59
		B	2.99	10.37	3.02	7.58
		C	3.27	10.30	3.04	7.52
	3	A	2.53	12.23	4.18	7.93
		B	2.55	12.13	4.16	7.93
		C	2.54	11.71	4.02	7.96
	4	A	3.59	12.11	4.41	8.40
		B	3.81	12.17	4.59	8.23
		C	4.18	11.87	4.34	8.39
	5	A	2.74	10.88	4.18	9.35
		B	2.74	10.95	4.19	9.28
		C	2.81	10.88	4.18	9.36
		Ave.	**2.84**	**10.76**	**3.55**	**7.70**
		Stdev.	**0.68**	**1.31**	**0.92**	**1.33**

Table S4: Calcification rates (three replicate measurements) under pulsed Sr-labelling aquaculture conditions for the inner layer of *K. rhytiphora*. Line # refer to blue, numbered lines in Supplementary Fig. 13 where growth measurements were obtained. LE 1 and LE 2 (both 6 days), refer to the first and second labelling periods while NE 1 (12 days) depicts normal Sr conditions between LE 1, LE 2, and NE 2 (either *6 days* or 12 days depending on specimen) describes growth at normal conditions after the last labelling event.

Sample ID:	Line #:	Rep.:	LE 1 [µm/6d]	NE 1 [µm/12d]	LE 2 [µm/6d]	NE 2 [µm/*6d*] or [µm/12d]
(A) K2-01	1	A	3.46	3.09	3.56	*3.69*
		B	3.44	3.13	3.50	*3.59*
		C	3.37	3.03	3.82	*3.66*
	2	A	3.23	3.80	4.06	*3.23*
		B	3.14	4.02	3.80	*3.20*
		C	3.29	3.80	3.92	*3.10*
	3	A	3.79	3.61	3.86	*3.29*
		B	3.73	3.67	3.86	*3.26*
		C	3.70	3.77	3.89	*3.39*
	4	A	3.64	3.99	4.08	*3.23*
		B	3.80	3.89	4.27	*3.20*
		C	3.61	4.05	4.27	*3.16*
	5	A	3.48	3.79	4.11	*3.29*
		B	3.38	3.86	4.24	*3.36*
		C	3.32	3.86	4.02	*3.36*
		Ave.	**3.49**	**3.69**	**3.95**	***3.33***
		Stdev.	**0.20**	**0.33**	**0.23**	***0.17***
(B) K2-02	1	A	4.26	4.08	3.61	*2.46*
		B	3.83	3.92	3.69	*2.45*
		C	3.91	3.82	3.77	*2.47*
	2	A	3.58	4.59	4.24	*2.94*
		B	3.32	4.73	4.10	*3.20*
		C	3.41	4.71	4.14	*3.32*
	3	A	3.92	3.92	3.74	*2.43*
		B	3.80	4.26	4.14	*2.63*
		C	3.43	3.99	3.72	*2.33*
	4	A	3.58	4.54	3.92	*2.37*
		B	3.48	4.40	4.03	*3.02*
		C	3.53	4.38	3.75	*2.29*
	5	A	3.29	4.40	4.03	*2.34*
		B	3.34	4.32	3.89	*2.45*
		C	3.28	4.27	4.07	*2.39*
		Ave.	**3.60**	**4.29**	**3.92**	***2.61***
		Stdev.	**0.28**	**0.28**	**0.19**	***0.33***
(C) K2-04	1	A	8.27	11.86	4.37	*3.49*
		B	8.17	12.19	4.59	*3.46*
		C	9.35	12.25	4.63	*3.15*
	2	A	3.49	9.89	4.47	*2.68*
		B	3.46	9.84	4.75	*2.54*
		C	3.15	9.59	4.75	*2.80*
	3	A	7.88	9.96	3.64	*3.39*
		B	7.82	9.87	3.64	*3.46*
		C	7.90	9.84	3.76	*2.78*
	4	A	7.50	9.77	4.23	*1.93*
		B	7.50	9.79	4.16	*1.83*
		C	7.86	9.78	4.35	*1.95*
	5	A	7.52	9.14	4.16	*1.66*
		B	7.50	9.49	4.25	*1.69*
		C	7.73	9.26	4.42	*1.52*
		Ave.	**7.01**	**10.17**	**4.28**	***2.55***
		Stdev.	**1.88**	**0.99**	**0.35**	***0.71***

Table S4 continued.

Sample ID:	Line #:	Rep.:	LE 1 [μm/6d]	NE 1 [μm/12d]	LE 2 [μm/6d]	NE 2 [μm/*6d*] or [μm/12d]
(D) K2-06	1	A	6.83	14.07	5.83	10.52
		B	6.71	14.35	5.98	10.48
		C	6.67	14.19	5.55	10.43
	2	A	6.52	14.19	5.40	10.40
		B	6.55	13.82	5.62	9.87
		C	6.56	14.18	5.42	9.73
	3	A	5.47	13.80	5.47	10.01
		B	5.49	13.80	5.50	10.11
		C	5.29	13.61	5.54	10.09
	4	A	5.87	13.06	5.79	10.52
		B	5.89	13.15	5.79	10.44
		C	5.88	12.99	5.27	10.09
	5	A	5.13	12.59	5.17	9.39
		B	5.42	12.72	5.22	9.35
		C	5.40	12.79	5.27	9.31
		Ave.	**5.98**	**13.55**	**5.52**	**10.05**
		Stdev.	**0.58**	**0.59**	**0.24**	**0.42**
(E) K2-08	1	A	5.99	11.10	4.11	7.56
		B	6.19	11.02	4.03	7.63
		C	6.06	11.09	4.04	7.62
	2	A	5.45	11.16	3.88	7.55
		B	5.40	11.03	3.82	7.56
		C	5.42	11.16	3.75	7.50
	3	A	5.04	10.79	3.30	7.48
		B	4.89	10.79	3.16	7.48
		C	4.88	10.72	3.32	7.41
	4	A	4.75	10.36	3.88	7.05
		B	4.89	10.20	3.95	7.19
		C	4.82	10.22	3.73	7.06
	5	A	4.76	10.44	3.31	6.91
		B	4.74	10.51	3.30	6.99
		C	4.89	10.44	3.45	6.98
		Ave.	**5.21**	**10.74**	**3.67**	**7.33**
		Stdev.	**0.49**	**0.34**	**0.31**	**0.26**
(F) K2-10	1	A	14.19	22.83	6.12	14.67
		B	13.86	22.75	6.12	14.75
		C	13.96	22.74	6.27	14.76
	2	A	13.29	24.30	6.34	16.13
		B	13.41	24.19	6.22	16.01
		C	13.49	24.31	6.32	16.03
	3	A	11.76	25.66	6.96	16.52
		B	11.74	25.88	7.07	16.53
		C	11.75	25.98	6.74	16.31
	4	A	12.72	25.66	6.41	16.85
		B	12.72	25.56	6.42	16.85
		C	12.62	25.44	6.52	16.86
	5	A	12.41	25.89	6.75	16.97
		B	12.40	25.89	6.75	17.07
		C	12.73	25.89	6.65	17.18
		Ave.	**12.87**	**24.86**	**6.51**	**16.23**
		Stdev.	**0.78**	**1.20**	**0.29**	**0.83**

Table S4 continued.

Sample ID:	Line #:	Rep.:	LE 1 [μm/6d]	NE 1 [μm/12d]	LE 2 [μm/6d]	NE 2 [μm/*6d*] or [μm/12d]
(G) K2-11	1	A	6.64	11.23	4.66	8.05
		B	6.50	11.36	4.24	7.82
		C	6.49	11.36	4.52	7.97
	2	A	6.57	11.45	4.44	7.83
		B	6.71	11.51	4.38	7.83
		C	6.63	11.52	4.31	7.62
	3	A	6.21	11.86	4.59	7.41
		B	6.42	11.86	4.52	7.55
		C	6.23	11.85	4.45	7.62
	4	A	6.84	11.64	4.30	7.20
		B	6.91	11.57	4.30	7.13
		C	6.77	11.71	4.37	7.20
	5	A	7.20	11.99	4.16	7.41
		B	6.91	11.85	4.12	7.48
		C	6.91	11.78	4.16	7.55
		Ave.	**6.66**	**11.64**	**4.37**	**7.58**
		Stdev.	**0.26**	**0.22**	**0.16**	**0.27**
(H) K2-14	1	A	6.42	30.16	10.91	15.42
		B	6.06	29.80	11.05	15.40
		C	5.99	30.23	10.84	15.76
	2	A	5.92	30.16	9.42	15.20
		B	6.07	30.14	9.49	14.83
		C	6.21	30.16	9.27	15.05
	3	A	7.21	31.03	8.84	14.12
		B	7.35	30.96	8.84	14.19
		C	7.20	30.96	8.77	13.98
	4	A	8.35	29.95	7.70	13.90
		B	8.20	30.23	7.63	14.26
		C	8.56	29.95	7.70	14.05
	5	A	8.63	30.37	8.25	14.55
		B	8.84	30.02	8.27	14.40
		C	8.77	29.95	8.20	14.48
		Ave.	**7.32**	**30.27**	**9.01**	**14.64**
		Stdev.	**1.11**	**0.38**	**1.12**	**0.58**

References

Pérez-Huerta, A., Cuif, J.-P., Dauphin, Y., and Cusack, M.: Crystallography of calcite in pearls, European Journal of Mineralogy, 26, 507–516, 2014.

Váczi, T.: A new, simple approximation for the deconvolution of instrumental broadening in spectroscopic band profiles, Applied spectroscopy, 68, 1274–1278, 2014.